International Conference on Textile Composites and Inflatable Structures
STRUCTURAL MEMBRANES 2011
E. Oñate, B. Kröplin and K.-U.Bletzinger (Eds)

MULTISCALE SEQUENTIALLY-COUPLED FSI COMPUTATION IN PARACHUTE MODELING

KENJI TAKIZAWA*, SAMUEL WRIGHT†, JASON CHRISTOPHER† AND TAYFUN E. TEZDUYAR†

*Department of Modern Mechanical Engineering and
Waseda Institute for Advanced Study, Waseda University
1-6-1 Nishi-Waseda, Shinjuku-ku, Tokyo 169-8050, JAPAN

†Mechanical Engineering, Rice University – MS 321
6100 Main Street, Houston, TX 77005, USA

Key words: Fluid–structure interaction, Ringsail parachute, Space–time technique, Geometric porosity, Multiscale FSI techniques, Membrane stresses

Abstract. We describe how the spatially multiscale Sequentially-Coupled Fluid–Structure Interaction (SCFSI) techniques we have developed, specifically the "SCFSI M2C", which is spatially multiscale for the structural mechanics part, can be used for increasing the accuracy of the membrane and cable structural mechanics solution in parachute FSI computations. The SCFSI M2C technique is used here in conjunction with the Stabilized Space–Time FSI (SSTFSI) technique, which was developed and improved over the years by the Team for Advanced Flow Simulation and Modeling (T★AFSM) and serves as the core numerical technology, and a number of special parachute FSI techniques developed by the T★AFSM in conjunction with the SSTFSI technique.

1 INTRODUCTION

The spatially multiscale Sequentially-Coupled Fluid–Structure Interaction (SCFSI) techniques were introduced in [1] as spatially multiscale for the fluid mechanics part, which is called "SCFSI M1C", and then in [2] as spatially multiscale for the structural mechanics part, which is called "SCFSI M2C". In SCFSI M2C, the time-dependent flow field is first computed with the (fully) coupled FSI (CFSI) technique and a relatively coarser structural mechanics mesh, followed by a structural mechanics computation with a more refined mesh, with the time-dependent interface stresses coming from the previously carried out CFSI computation. With this technique, the FSI computational effort is reduced where it is not needed, and the accuracy of the structural mechanics computation is increased where we need accurate, detailed structural mechanics computations, such as computing the fabric stresses. We can do this because the coarse mesh is sufficient for the purpose of FSI computations, and using more refined meshes does not change the FSI results that much. However, mesh refinement does make a difference in detailed structural mechanics computation.

The SCFSI M1C and SCFSI M2C techniques have been used in conjunction with the the Stabilized Space–Time FSI (SSTFSI) technique, which was developed and improved over the years by the Team for Advanced Flow Simulation and Modeling (T★AFSM) and serves as the core numerical technology, and special techniques developed in conjunction with the SSTFSI technique. In the case of the SCFSI M2C technique, the applications have been in parachute FSI modeling, and therefore the special techniques developed in conjunction with the SSTFSI technique have targeted parachute computations.

The SSTFSI technique was introduced in [3]. It is based on the new-generation Deforming-Spatial-Domain/Stabilized Space–Time (DSD/SST) formulations, which were also introduced in [3], increasing the scope and performance of the DSD/SST formulations developed earlier [4, 5, 6, 7] for computation of flows with moving boundaries and interfaces, including FSI. This core technology was used in a large number of parachute FSI computations (see, for example, [3, 8, 9, 2, 10, 11, 12, 13]). The FSI coupling is handled with the direct and quasi-direct FSI coupling techniques, which were introduced in [14] and are generalizations of the monolithic solution techniques to cases with incompatible fluid and structure meshes at the interface. They remain robust in computations where the structure is light compared to the fluid masses involved in the dynamics of the FSI problem, which is the case in parachute modeling. They were used in a large number of parachute FSI computations (see, for example, [3, 8, 9, 2, 10, 11, 12, 13]).

Computer modeling of large ringsail parachutes by the T★AFSM was first reported in [8, 9]. The geometric challenge created by the construction of the canopy from "rings" and "sails" with hundreds of ring gaps and sail slits has been addressed with the Homogenized Modeling of Geometric Porosity (HMGP) [8], adaptive HMGP [2] and a new version of the HMGP that is called "HMGP-FG" [10]. These special techniques make the problem tractable. Additional special techniques the T★AFSM introduced in the context of ringsail parachutes include the FSI Geometric Smoothing Technique (FSI-GST) [3], Separated Stress Projection (SSP) [8], "symmetric FSI" technique [2], a method that accounts for the fluid forces acting on structural components (such as parachute suspension lines) that are not expected to influence the flow [2], and other interface projection techniques [15].

The SCFSI M2C technique was used in [2] and [11] for increasing the accuracy of the membrane and cable structural mechanics solution in parachute FSI computations, and we provide in this paper an overview of those computations.

2 MULTISCALE SCFSI M2C COMPUTATIONS

2.1 Structural mechanics solution for the reefed stage

In [2] the SCFSI M2C technique was used for increasing the accuracy of the structural mechanics solution for the parachute reefed to approximately 13%. During the descent of a spacecraft, the parachute skirt is initially constricted to reduce forces on the parachute structure and the crew, and this is called the reefed stage. The skirt diameter is constrained using a reefing line, with length characterized by the "reefing ratio": $\tau_{REEF} = D_{REEF}/D_0$, where D_{REEF} is the reefed skirt diameter and D_0 is the parachute nominal diameter. Starting with the fully open parachute geometry, which is relatively easier to compute, an incremental shape determination approach based on gradually shortening the reefing line was used in [2] to compute the parachute shape at reefed configurations. Because the objective was just to determine the parachute shape, the symmetric FSI technique was used.

The coarse structure mesh used in the CFSI computation consists of 31,122 nodes and 26,320 four-node quadrilateral membrane elements, 12,441 two-node cable elements, and one payload point mass. The membrane part of the structure forms the structure interface and has 29,600 nodes. More information on the computational conditions, including the homogenized-porosity values, fluid mechanics mesh, time-step size and iteration numbers and computational steps followed, can be found in [2]. Figure 1 shows the structural mechanics solution for the parachute reefed to $\tau_{REEF} = 13\%$ (approximately).

Figure 1: Structural mechanics solution for the parachute reefed to $\tau_{REEF} = 13\%$ (approximately), obtained with the CFSI computation and the coarse structure mesh.

In the SCFSI M2C computation, the interface stresses were extracted from the CFSI computation described above and were used in a structural mechanics computation with a more refined mesh. The interface stress projected to the structure consists of only the pressure component of the interface stress, and the SSP technique is used for the projection. The refined structure mesh has 128,882 nodes and 119,040 four-node quadrilateral membrane elements, 23,001 two-node cable elements and one payload point mass. The membrane part of the structure forms the structure interface and has 127,360 nodes. At this reefed configuration, the interface stresses obtained in the symmetric FSI computation do not have a significantly dynamic nature, and therefore the time-averaged values were used.

As a related technique, a "cable symmetrization" procedure to be applied to the canopy cables during the structural mechanics computation with the more refined mesh was proposed in [2]. In this procedure, it was proposed that for the cable nodes at each latitude, the tangential component of the displacement is set to zero, and the radial and axial components are set to the average values for that latitude. This can be done as frequently as every nonlinear iteration, or as few as just once. In the computation reported in [2], it was done just once and that was during the starting phase of the computation. Also, in the computation reported in [2], the actual symmetrization procedure used was a close approximation to the proposed one. Figure 2 shows the canopy cables before and after symmetrization. In addition to and following that symmetrization, the cable

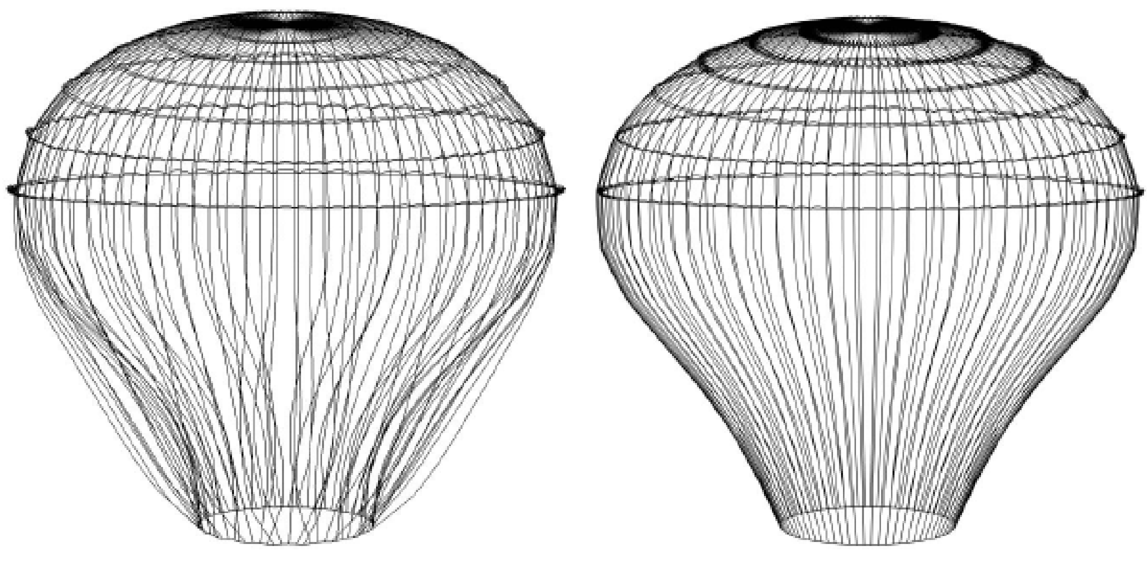

Figure 2: Structural mechanics solution for the parachute reefed to $\tau_{REEF} = 13\%$ (approximately). Canopy cables before (left) and after (right) symmetrization.

positions are fixed and the computation is continued until the membrane parts of the canopy structure settle. After that we release all the structural nodes (except for the payload) and compute until the solution settles. Figure 3 shows the structural mechanics solution obtained with the SCFSI M2C computation and the refined mesh. Figure 4

Figure 3: Structural mechanics solution for the parachute reefed to $\tau_{REEF} = 13\%$ (approximately), obtained with the SCFSI M2C computation and the refined structure mesh.

shows the structural mechanics solution obtained with the SCFSI M2C computation and a picture from a NASA drop test.

2.2 Fabric stress computations

It was shown in [11] that the SCFSI M2C technique can be used for computing the fabric stresses more accurately by increasing the structural mesh refinement after the CFSI computation is carried out with a coarse mesh. It was also shown how the SCFSI M2C technique can be used for computing the fabric stress more accurately by adding the "vent hoop" after the FSI computation is carried out without it. The vent hoop is a reinforcement cable placed along the circumference of the vent. Again, we can do this because the structural model without the vent hoop is sufficient for the purpose of FSI computations, and including the vent hoop does not change the FSI results that much. However it makes a large difference in the fabric stresses near the vent.

In the tests carried out in [11] with the SCFSI M2C technique, the interface stresses are extracted from the FSI computation reported in [10] (for the case where the horizontal speed of the payload is instantaneously hiked to 20 ft/s to emulate the swinging motion). The stress projected to the structure consists of only the pressure component of the interface stress, and the SSP technique is used for the projection. Also, to expedite the tests,

Figure 4: Structural mechanics solution for the parachute reefed to $\tau_{REEF} = 13\%$ (approximately). Left: obtained with the SCFSI M2C computation and the refined structure mesh. Right: picture from a NASA drop test.

in [11] a time-averaged, circumferentially symmetric pressure was applied to the structure. The coarse structure mesh for the canopy has 29,200 nodes, 26,000 four-node membrane elements, and 10,920 two-node cable elements. The fine mesh has 115,680 nodes, 108,480 four-node membrane elements, and 21,640 two-node cable elements. Adding the vent hoop increases the number of cable elements by 80. Figures 5 and 6 show the coarse and fine meshes for one gore.

The cases with and without a vent hoop were computed in [11] using both meshes, resulting in a total of four test cases. Additional information on the computational conditions, including the time-step size and iteration numbers and computational steps followed, can be found in [11]. Figures 7 and 8 show the fabric (maximum principal) tension for the coarse and fine meshes with no vent hoop. Figures 9 and 10 show the fabric tension for the coarse and fine meshes with a vent hoop. Figures 11 and 12 show, for the cases without and with a vent hoop, the maximum fabric tension for each ring and sail, computed with the coarse and fine meshes.

3 CONCLUDING REMARKS

We showed that the spatially multiscale SCFSI techniques we have developed, specifically the SCFSI M2C technique, which is spatially multiscale for the structural mechanics part, can be used very effectively for increasing the accuracy of the membrane and cable structural mechanics solution in parachute FSI computations. In the computations reported here, the SCFSI M2C technique is used in conjunction with the SSTFSI tech-

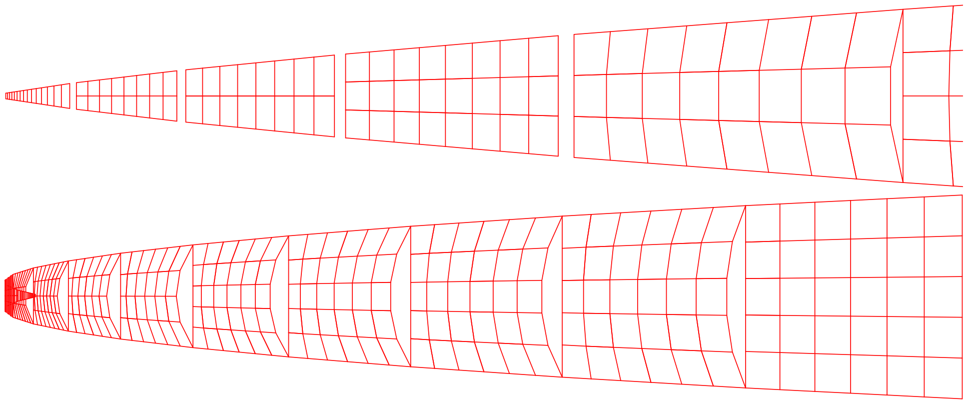

Figure 5: Coarse structure mesh for one gore.

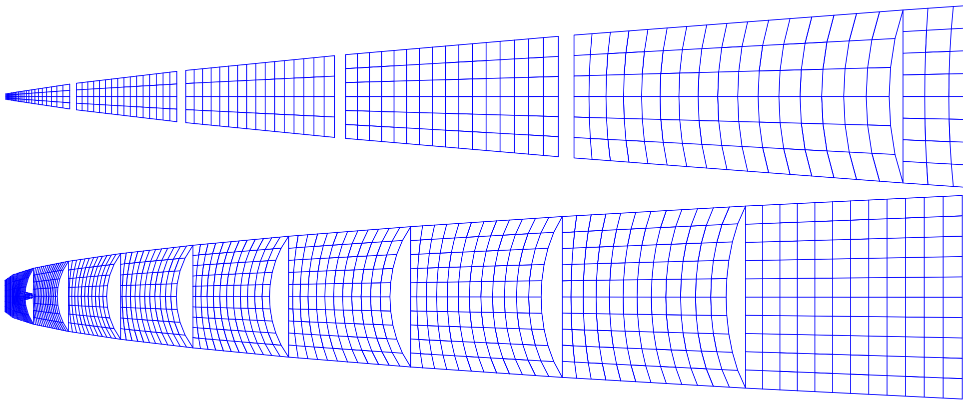

Figure 6: Fine structure mesh for one gore.

nique, which serves as the core numerical technology, and a number of special parachute FSI techniques developed in conjunction with the SSTFSI technique. We presented results from computations where the SCFSI M2C technique is used for increasing the accuracy of the structural mechanics solution for the parachute reefed to approximately 13%, for computing the fabric stresses more accurately for a fully open parachute, and for computing the fabric stress more accurately when a vent hoop is added to the parachute structure.

ACKNOWLEDGMENT

This work was supported by NASA Grant NNX09AM89G, and also in part by the Rice Computational Research Cluster funded by NSF Grant CNS-0821727.

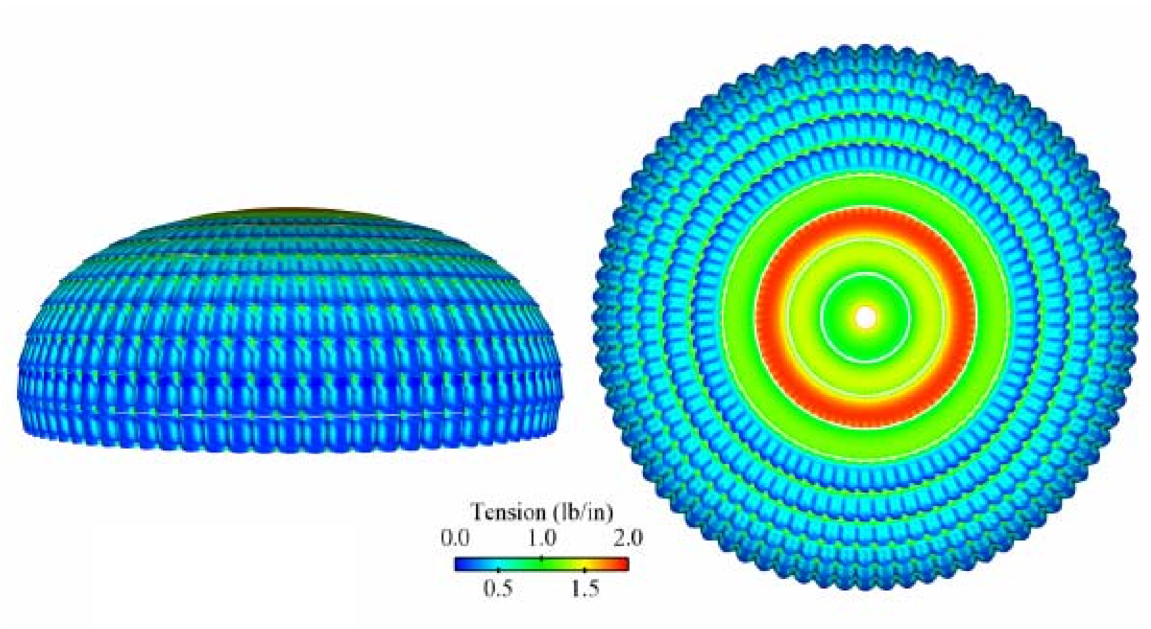

Figure 7: Fabric tension for the coarse mesh with no vent hoop.

REFERENCES

[1] T.E. Tezduyar, M. Schwaab, and S. Sathe, "Sequentially-Coupled Arterial Fluid–Structure Interaction (SCAFSI) technique", *Computer Methods in Applied Mechanics and Engineering*, **198** (2009) 3524–3533, doi: 10.1016/j.cma.2008.05.024.

[2] T.E. Tezduyar, K. Takizawa, C. Moorman, S. Wright, and J. Christopher, "Space–time finite element computation of complex fluid–structure interactions", *International Journal for Numerical Methods in Fluids*, **64** (2010) 1201–1218, doi: 10.1002/fld.2221.

[3] T.E. Tezduyar and S. Sathe, "Modeling of fluid–structure interactions with the space–time finite elements: Solution techniques", *International Journal for Numerical Methods in Fluids*, **54** (2007) 855–900, doi: 10.1002/fld.1430.

[4] T.E. Tezduyar, "Stabilized finite element formulations for incompressible flow computations", *Advances in Applied Mechanics*, **28** (1992) 1–44, doi: 10.1016/S0065-2156(08)70153-4.

[5] T.E. Tezduyar, M. Behr, and J. Liou, "A new strategy for finite element computations involving moving boundaries and interfaces – the deforming-spatial-domain/space–time procedure: I. The concept and the preliminary numerical tests", *Computer*

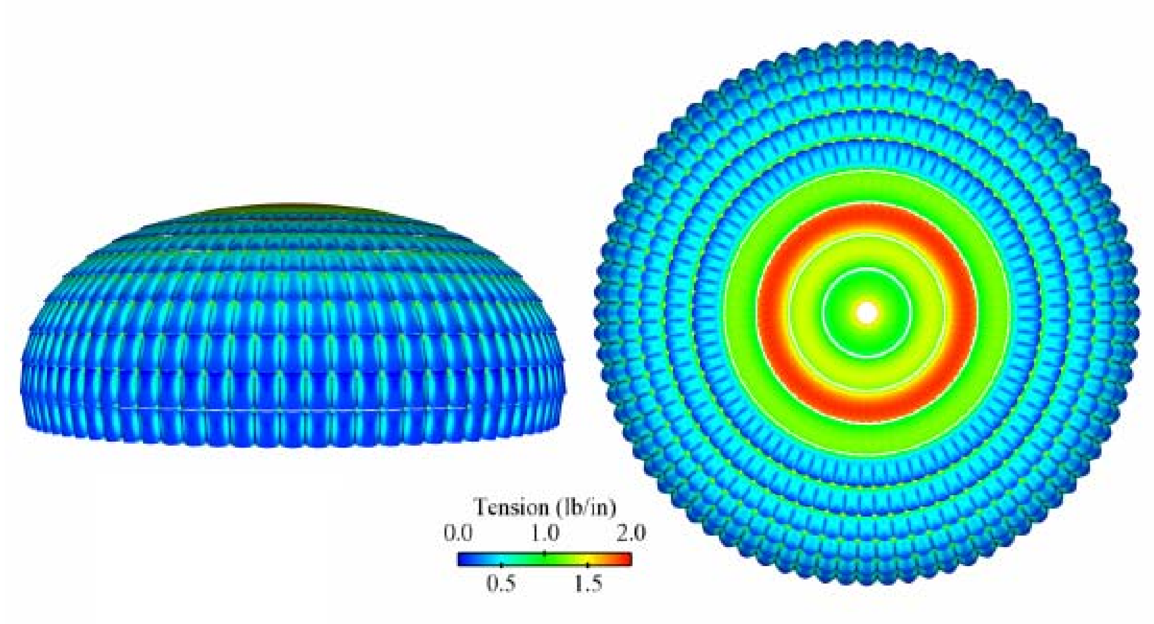

Figure 8: Fabric tension for the fine mesh with no vent hoop.

Methods in Applied Mechanics and Engineering, **94** (1992) 339–351, doi: 10.1016/0045-7825(92)90059-S.

[6] T.E. Tezduyar, M. Behr, S. Mittal, and J. Liou, "A new strategy for finite element computations involving moving boundaries and interfaces – the deforming-spatial-domain/space–time procedure: II. Computation of free-surface flows, two-liquid flows, and flows with drifting cylinders", *Computer Methods in Applied Mechanics and Engineering*, **94** (1992) 353–371, doi: 10.1016/0045-7825(92)90060-W.

[7] T.E. Tezduyar, "Computation of moving boundaries and interfaces and stabilization parameters", *International Journal for Numerical Methods in Fluids*, **43** (2003) 555–575, doi: 10.1002/fld.505.

[8] T.E. Tezduyar, S. Sathe, J. Pausewang, M. Schwaab, J. Christopher, and J. Crabtree, "Interface projection techniques for fluid–structure interaction modeling with moving-mesh methods", *Computational Mechanics*, **43** (2008) 39–49, doi: 10.1007/s00466-008-0261-7.

[9] T.E. Tezduyar, S. Sathe, J. Pausewang, M. Schwaab, J. Christopher, and J. Crabtree, "Fluid–structure interaction modeling of ringsail parachutes", *Computational Mechanics*, **43** (2008) 133–142, doi: 10.1007/s00466-008-0260-8.

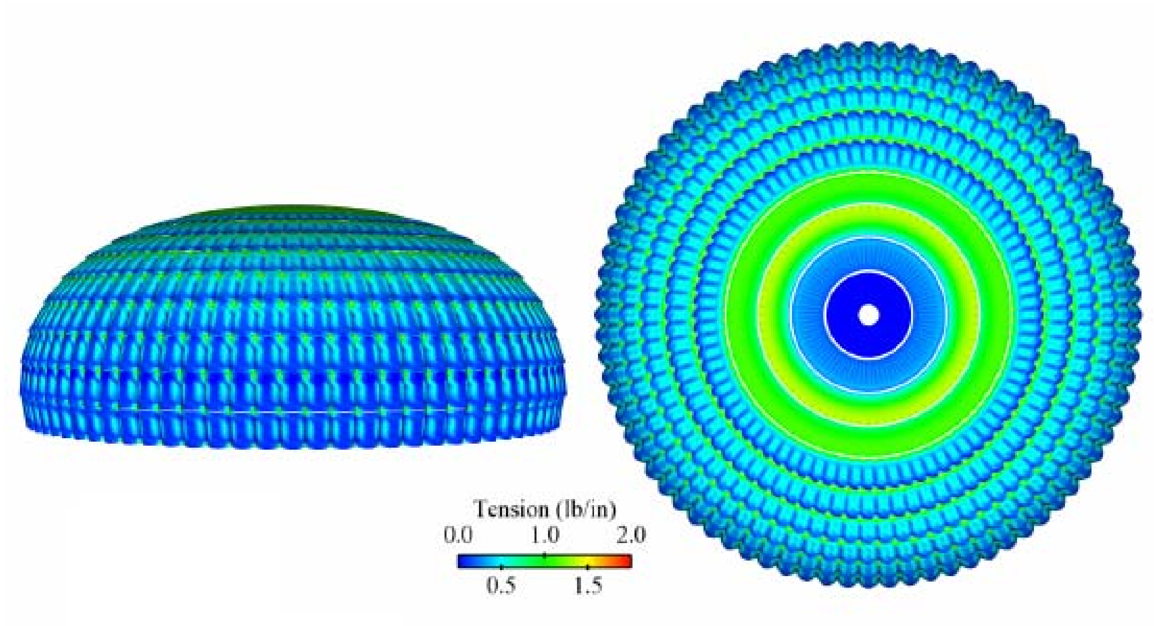

Figure 9: Fabric tension for the coarse mesh with a vent hoop.

[10] K. Takizawa, C. Moorman, S. Wright, T. Spielman, and T.E. Tezduyar, "Fluid–structure interaction modeling and performance analysis of the Orion spacecraft parachutes", *International Journal for Numerical Methods in Fluids*, **65** (2011) 271–285, doi: 10.1002/fld.2348.

[11] K. Takizawa, S. Wright, C. Moorman, and T.E. Tezduyar, "Fluid–structure interaction modeling of parachute clusters", *International Journal for Numerical Methods in Fluids*, **65** (2011) 286–307, doi: 10.1002/fld.2359.

[12] K. Takizawa, T. Spielman, and T.E. Tezduyar, "Space–time FSI modeling and dynamical analysis of spacecraft parachutes and parachute clusters", *Computational Mechanics*, published online, DOI: 10.1007/s00466-011-0590-9, April 2011, doi: 10.1007/s00466-011-0590-9.

[13] K. Takizawa, T. Spielman, C. Moorman, and T.E. Tezduyar, "Fluid–structure interaction modeling of spacecraft parachutes for simulation-based design", *Journal of Applied Mechanics*, to appear, 2011.

[14] T.E. Tezduyar, S. Sathe, R. Keedy, and K. Stein, "Space–time finite element techniques for computation of fluid–structure interactions", *Computer Methods in Applied Mechanics and Engineering*, **195** (2006) 2002–2027, doi: 10.1016/j.cma.2004.09.014.

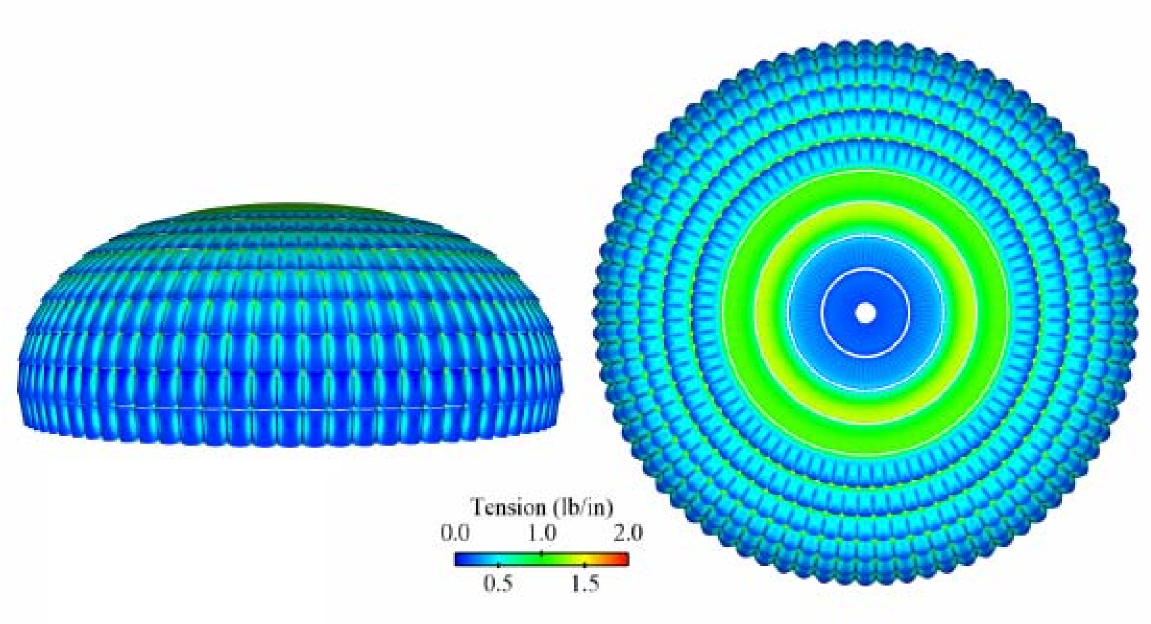

Figure 10: Fabric tension for the fine mesh with a vent hoop.

[15] K. Takizawa, C. Moorman, S. Wright, J. Christopher, and T.E. Tezduyar, “Wall shear stress calculations in space–time finite element computation of arterial fluid–structure interactions”, *Computational Mechanics*, **46** (2010) 31–41, doi: 10.1007/s00466-009-0425-0.

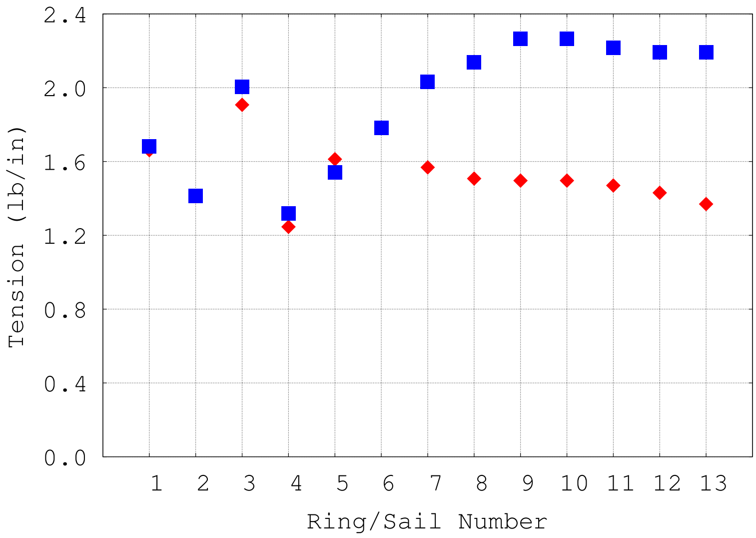

Figure 11: Maximum fabric tension for each ring and sail for the case with no vent hoop. Coarse mesh results denoted with red diamonds and fine mesh results denoted with blue squares.

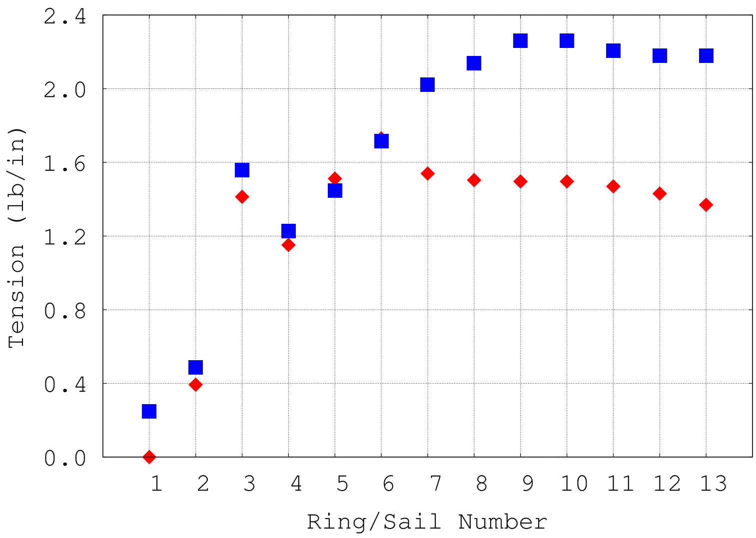

Figure 12: Maximum fabric tension for each ring and sail for the case with a vent hoop. Coarse mesh results denoted with red diamonds and fine mesh results denoted with blue squares.